# The Influence of Microstructure and Strain Rate on the Compressive Deformation Behavior of Ti-6Al-4V

A.J. WAGONER JOHNSON, C.W. BULL, K.S. KUMAR, and C.L. BRIANT

This article reports on a study of deformation of Ti-6Al-4V in compression. In particular, two different microstructures, the equiaxed microstructure and the Widmanstätten microstructure, were generated from the same parent material and their properties were measured. The results show that at small strains, the mechanical response of samples with these microstructures is similar. The yield strength and the flow stress at a 0.05 true strain have similar values; these increase with increasing strain rate over the range of 0.1 to 1000 $s^{-1}$. However, samples with the Widmanstätten microstructure failed at a smaller strain than their counterparts with the equiaxed microstructure, and this difference increased with increasing strain rate. Examination of cross sections of samples deformed to different levels of strain showed that the deformation was inhomogeneous. As the sample barreled, the deformation built up on the surfaces of two cones of material whose apices met in the center of the sample. Cracks formed in the corners of the samples and propagated in toward the center. In samples with the equiaxed microstructure, short cracks and voids formed, but they were usually blunted at the grain boundaries. Long cracks were only observed immediately before failure. In samples with the Widmanstätten microstructure, cracks could grow within the laths more easily, and, as a result, longer cracks formed at lower strains. We propose that this difference leads to the differences in the failure strains for these two microstructures. Finally, examination of data in the literature, along with our own results, indicates that the interstitial content plays an important role in determining the yield stress of the material.

## I. INTRODUCTION

THE titanium alloy Ti-6Al-4V (Ti64) has been used for high-performance applications, including those in the aerospace and defense industries, for over 20 years.[1] More recently, this alloy has been considered for use in ballistic applications, in which it would experience large compressive strains and nonuniform deformation.[1–4] Although a number of investigators have documented the properties of the material in compression,[4–9] the effects of microstructure on deformation and fracture have not been comprehensively described.

Two commonly used microstructures of Ti64 are the equiaxed and the Widmanstätten structures. To date, no single study has carefully compared the mechanical response in compression of these two microstructures using material prepared from the same parent ingot. Thus, if one seeks to compare the response of these two microstructures using the data in the literature, other factors that vary from one study to another, such as interstitial content, details of the test method, and overall processing history of the material, could affect the conclusions.[4–9] For example, a compilation of the literature data shows that the reported values of the yield strength vary by approximately 400 MPa for a given strain rate, and the failure strains for the Widmanstätten microstructure alone vary between approximately 10 and 30 pct.[5,6,7] In addition, there has been debate about whether adiabatic shear bands play a role in the final failure process.[2,3,8,10,11]

To reconcile these differences, we have examined the compressive behavior of this material using samples with the equiaxed or Widmanstätten structures, created from the same parent material. The results show that the yield stress as well as the flow stress at a 0.05 true strain are similar for the two microstructures for strain rates ranging from 0.1 to 1000 $s^{-1}$. However, the microstructure and the test strain rate play an important role in the evolution of inhomogeneous deformation and markedly affect the failure strain of the material. More specifically, samples with the Widmanstätten microstructure failed at lower strains than did samples with the equiaxed microstructure, and this difference became greater with increasing strain rate. Finally, discrepancies in the yield strength among the previous studies can be explained by the different interstitial contents of the materials.

## II. EXPERIMENTAL PROCEDURE

Prealloyed Ti-6Al-4V powder ($-325$ mesh) was hot pressed at 1000 °C and isothermally forged in vacuum ($5 \times 10^{-5}$ Torr, maximum) in the $\alpha + \beta$–phase field at 875 °C. Forging resulted in a height reduction from 20 to 6.7 mm. The Widmanstätten microstructure was obtained by heat treating vacuum-encapsulated samples at 1100 °C in the $\beta$-phase field for 1 hour and furnace cooling them to room temperature. Chemical analysis after complete processing of the material showed that the interstitial content was 0.18 O, 0.093 C, and 0.021 N, with all values in wt pct.

We performed compression tests at strain rates of 0.1, 1.0,

A.J. WAGONER JOHNSON, formerly Graduate Student, Division of Engineering, Brown University, is Research Scientist and Lecturer, Department of Mechanical and Industrial Engineering, University of Illinois at Urbana–Champaign, Urbana, IL 61801. C.W. BULL, Senior Lecturer, K.S. KUMAR, Professor of Engineering, and C.L. BRIANT, Otis E. Randall University Professor, are with the Division of Engineering, Brown University, Providence, RI 02912. Contact e-mail: Clyde_Briant@brown.edu
Manuscript submitted December 28, 2001.

and 10 $s^{-1}$ using a servohydraulic machine. Tests performed at these strain rates will be referred to as quasi-static in this article. The cylindrical samples used in these tests had an initial diameter of 6.35 mm and an initial height of 6.7 mm. Sample ends were lubricated with a silicon grease prior to testing. Load values were converted to true-stress values using the constant-volume criterion, which assumes that the sample deforms uniformly and remains a perfect cylinder. The temperature rise during compression testing was also measured on samples deformed at strain rates of 0.1 and 10 $s^{-1}$. A hole, approximately 1.5-mm deep and 0.5 mm in diameter, was drilled into each specimen at half height. A K-type thermocouple was inserted into the hole. Time, temperature, load, and displacement were recorded during these tests using a digital oscilloscope.

We used a Kolsky (or split-Hopkinson) bar[12–15] to test samples at a strain rate of approximately 1000 $s^{-1}$. The stress wave was initiated by impacting the incident bar with a projectile that was propelled by a gas gun; a momentum trap at the end of the transmitted bar was used to prevent sample reloading. Stress and strain information was obtained following standard procedures.[12,13] A dispersion correction was performed on the raw strain-time data following a procedure described by Follansbee and Frantz.[16]

Transmission electron microscopy (TEM) was used for a more detailed characterization of the undeformed microstructures. The deformed substructure of the equiaxed samples was also examined after compressing specimens to a strain of ~10 pct at strain rates of 0.1 and 1000 $s^{-1}$. The TEM foils were made parallel to the loading direction by grinding, dimpling, and ion milling 3 mm disks. Since Ti64 is highly susceptible to hydrogen contamination during TEM specimen preparation,[17,18,19] care was taken to minimize the amount of contact the specimen had with water. Samples deformed to strains greater than 10 pct were also examined using the optical microscope and scanning electron microscope (SEM). These samples were etched with an aqueous solution of 10 pct HF-40 pct $HNO_3$.

## III. RESULTS

As stated in the Introduction, the primary purpose of this article is to compare the compressive mechanical behavior of the equiaxed and Widmanstätten microstructures. Therefore, in this section, we first describe these two microstructures in their undeformed condition. We then present the mechanical-test data for these microstructures and follow that with an analysis of the deformed microstructure.

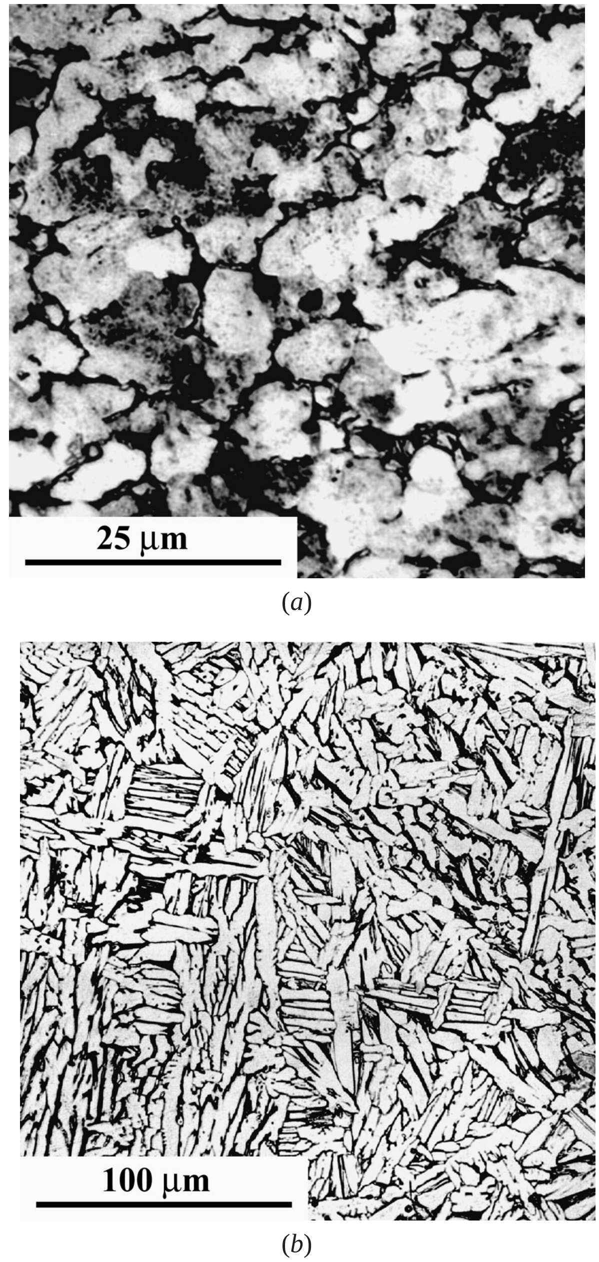


Fig. 1—Optical micrographs showing the (*a*) equiaxed and (*b*) Widmanstätten microstructures.

### A. *Undeformed Microstructures*

Optical micrographs of these two structures are shown in Figure 1. Both contained 18 pct $\beta$ phase at room temperature, as determined by optical metallography. The grain size of the equiaxed microstructure was approximately 8 $\mu$m, and the lath widths and lengths in the Widmanstätten structure were 10 to 12 $\mu$m and 25 to 50 $\mu$m, respectively.

Most $\alpha$ grains in the undeformed equiaxed microstructure had a low dislocation density. However, some were populated with dislocation networks or sub-boundaries, as shown in Figure 2(a). Equilibrium $\beta$ was located at grain boundaries, and a small amount of transformed $\beta$ was present at triple points. As previously reported,[20] transformed $\beta$ consists of $\beta$ and acicular $\alpha$, in which the $\alpha/\beta$ orientation relationship is $(110)_\beta//(0001)\alpha$ and $[111]_\beta//[1\ \bar{2}\ 10]_\alpha$. A micrograph of the transformed $\beta$ is shown in Figure 2(b), along with a diffraction pattern on the $[111]_\beta//[1\ \bar{2}\ 10]_\alpha$ zone axis in the inset.

The TEM of the Widmanstätten structure showed that the $\alpha$ phase here contained a higher dislocation density than that found in the $\alpha$ phase in the equiaxed structure. An example is shown in Figure 2(c). What was identified in the optical microscope as the dark $\beta$ phase had a lath width approximately 4 times smaller than that of the $\alpha$ phase. However, it was found that these laths were actually transformed $\beta$. An example is shown in Figure 2(d).

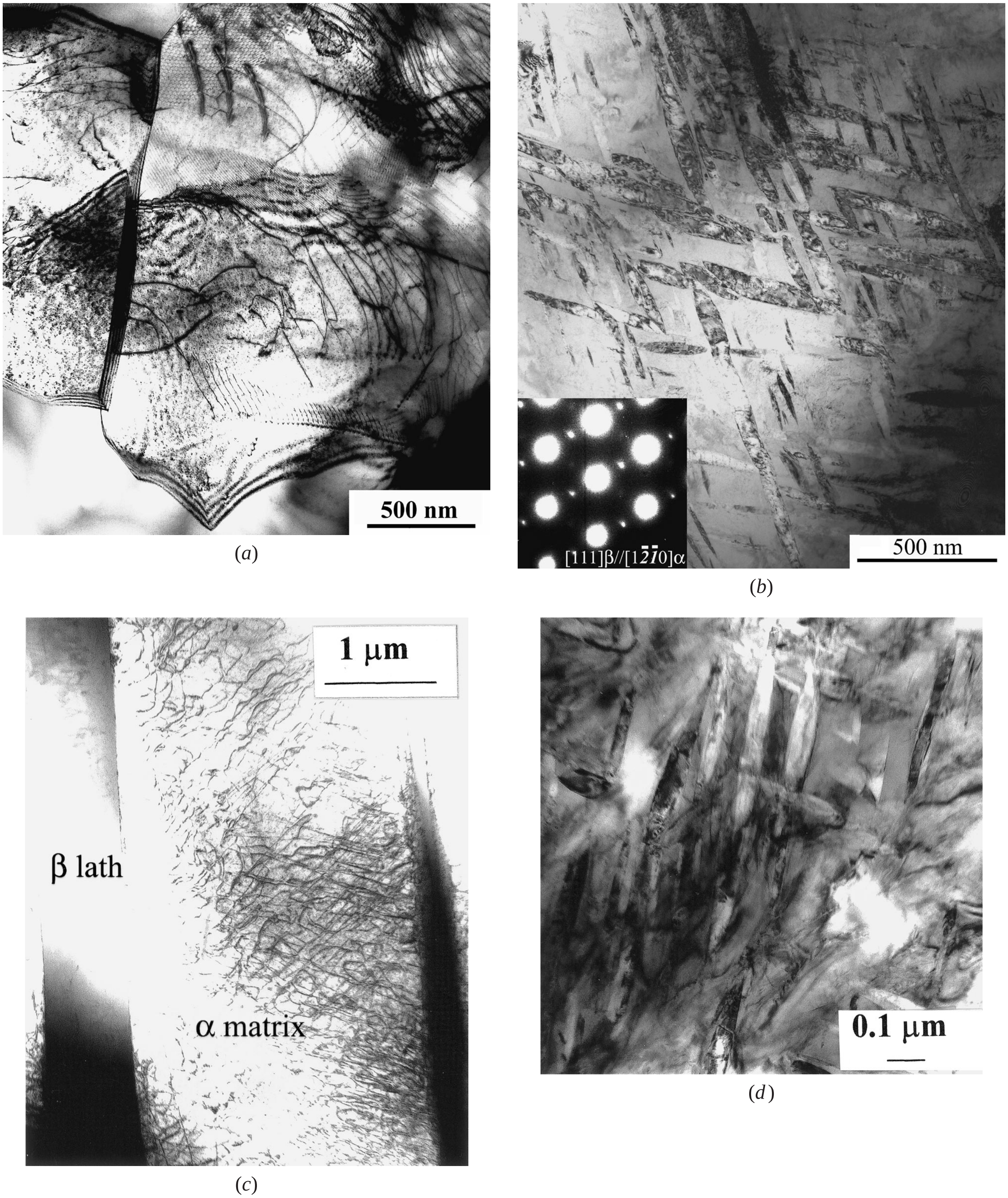


Fig. 2—Bright-field images of undeformed Ti64. (*a*) Dislocations within subgrains in the equiaxed microstructure. (*b*) Transformed-$\beta$ in the equiaxed microstructure and the corresponding selected area diffraction pattern on the $[111]_\beta//[1\,\bar{2}\,10]_\alpha$ zone axis. (*c*) Dislocation structures observed in the $\alpha$ phase in the Widmanstätten microstructure. (*d*) Transformed-$\beta$ in the Widmanstätten microstructure.

We also found that samples with the equiaxed microstructure contained the interface phase that has been reported to occur in this alloy.[17,18,19] These phases have previously been attributed to hydrogen contamination resulting from contact with water or electropolishing solution during foil preparation.[17] However, in this study, these phases were observed in samples that had been ion milled. They were more prominent in samples ion milled for especially long times or in older samples that had been stored in air. Efforts to produce foils of the equiaxed microstructure without the interface

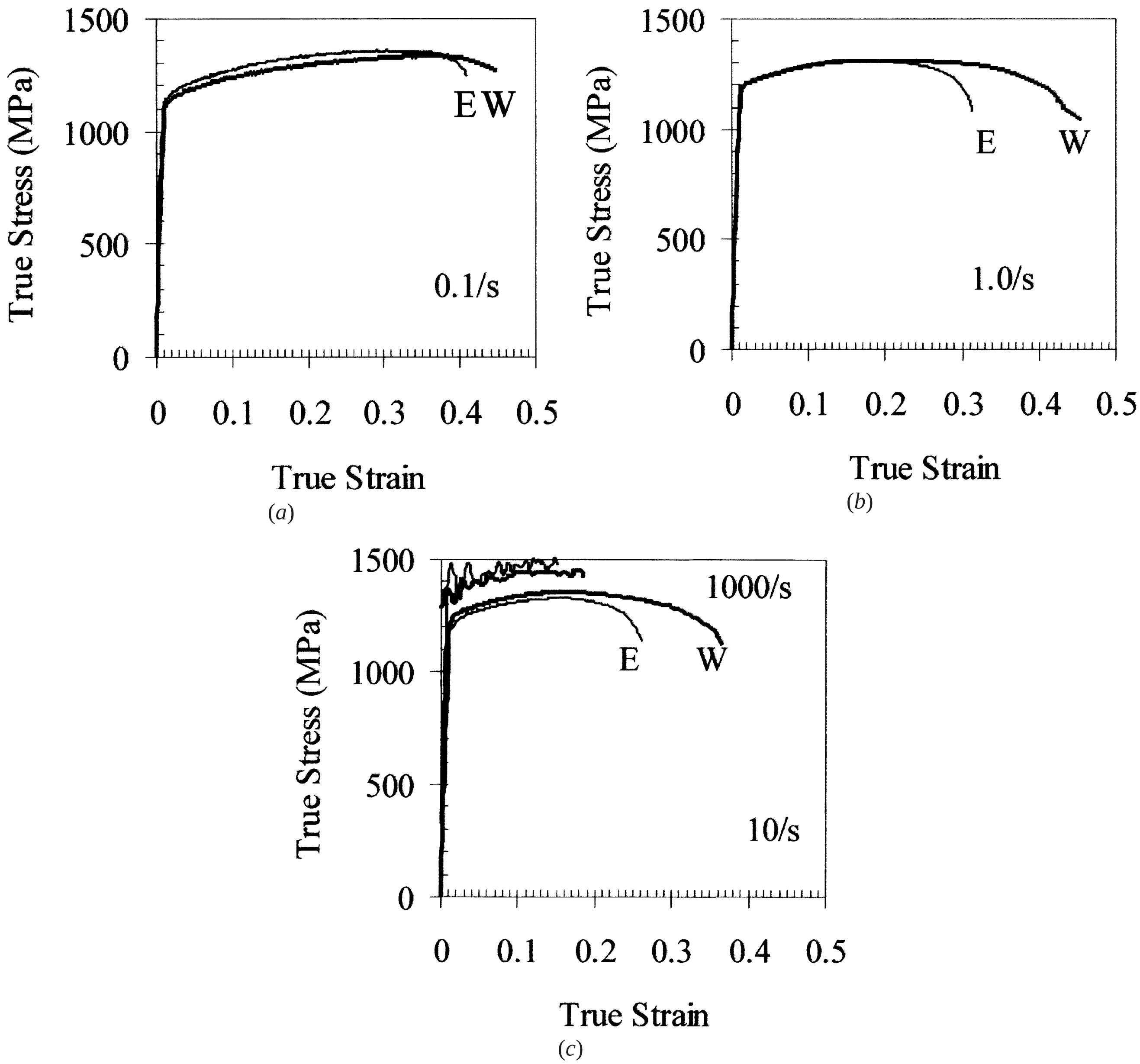


Fig. 3—True stress–true strain plots for samples tested in compression at different strain rates. In each figure, the thick line corresponds to sample with the equiaxed (*E*) microstructure and the thin line corresponds to samples with the Widmanstätten (*W*) microstructure. All samples tested at quasi-static strain rates were tested to failure. (*a*) Data for samples tested at 0.1 $s^{-1}$. (*b*) Data for samples tested at 1.0 $s^{-1}$. (*c*) Data for samples tested at 10 and 1000 $s^{-1}$.

phases were unsuccessful. No interface phases were observed in the foils of samples that had the Widmanstätten microstructure.

### B. *Compression-Test Results*

Compression tests were conducted at strain rates of 0.1, 1, 10, and 1000 $s^{-1}$. Figure 3 presents the true stress–true strain curves for both the Widmanstätten and equiaxed structures. Figures 3(a) and (b) show results for tests conducted at 0.1 and 1 $s^{-1}$, respectively. Figure 3(c) shows results from tests conducted at 10 and 1000 $s^{-1}$. The tests that were performed at strain rates of 0.1, 1, and 10 $s^{-1}$ were all continued to failure. Note that in the test performed at the dynamic strain rate (1000 $s^{-1}$), the total plastic strain was significantly less than that obtained in the other tests. These specimens could not be tested to failure due to constraints in the design of the Kolsky bar. Figure 4 summarizes the effect of test strain rate on the 0.2 pct offset yield stress for the quasi-static tests and the flow stress at 0.05 true strain for the quasi-static and high-strain-rate tests for both microstructures.

A number of important observations can be made from these mechanical-property results. First, the yield and flow stress increase linearly with strain rate on a log scale; this results is consistent with previous investigations.[2,5,6,9] Second, a true-stress maximum is present in the data obtained in quasi-static tests. The maximum at 0.1 $s^{-1}$ is followed immediately by specimen failure; however, the maxima observed at strain rates of 1.0 and 10 $s^{-1}$ are followed by a softening of the material. As shown in Section IV, this maximum appears to be a result of local heating. In Figure

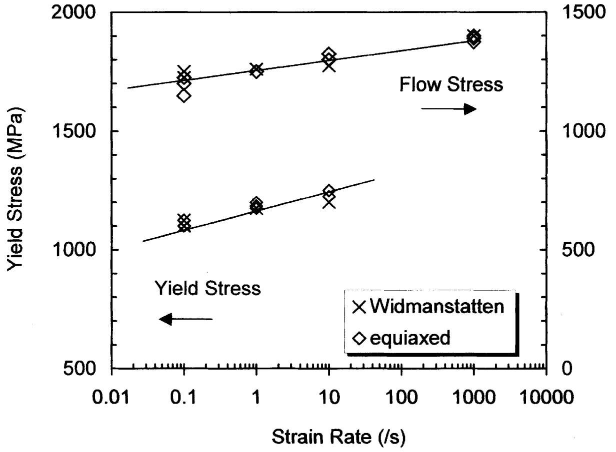

Fig. 4—The 0.2 pct yield stress and the flow stress at 0.05 true plastic strain plotted as a function of strain rate for samples with both the equiaxed and Widmanstätten microstructures.

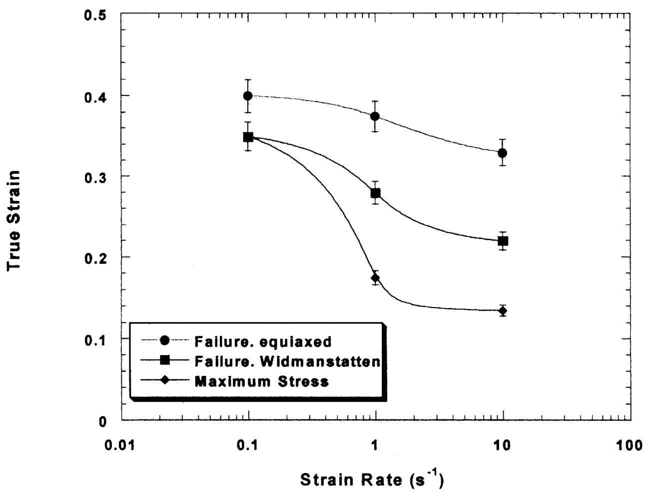

Fig. 5—The true strain at various points on the stress strain curve plotted as a function of strain rate. The particular points included on the plot are the failure strains for samples with both the equiaxed and Widmanstätten microstructures and the true strain at which the maximum in the true stress–true strain curve was observed.

5, we have plotted, for both microstructures, the true strain at the true-stress maximum as a function of strain rate. Note that the maximum in true stress for a given strain rate occurs at the same strain for both microstructures. Also included in the figure is the failure strain plotted as a function of strain rate. At each strain rate, the sample with the Widmanstätten microstructure fails at a lower strain than the one with the equiaxed structure, and the difference between failure strains increases with increasing strain rate in the quasi-static regime.

### C. *Deformed Microstructures*

In order to understand the overall deformation of these samples, we found it helpful to examine etched cross sections of deformed samples using both the optical microscope and the SEM. In general, we found that in the cross sections parallel to the loading direction, the deformation was nonuniform and was concentrated into two bands that formed an "X" on the polished section. In three dimensions, this pattern would be the surfaces of two cones of deformation with their apices in the center of the sample. Such deformation is typical of material that has undergone barreling during compression testing.

More detailed information could be obtained by examining samples deformed to different levels of strain at different strain rates. We first consider samples with the equiaxed microstructure deformed to 0.09, 0.28, and 0.33 true strain, respectively, at a strain rate of 0.1 s$^{-1}$. The sample deformed to 0.09 strain showed no microstructural evidence of nonuniform deformation. In the samples deformed to 0.28 and 0.33 strains, a region of deformed material was visible in the corners of the cross section. An example is shown in Figure 6(a). Examination of these samples in the SEM showed that voids were also present in these regions, with more being present in the sample deformed to a strain of 0.33. An example of these voids is shown in Figure 6(b). These voids tended to be isolated and had not connected to form a long crack.

We now compare the damage in samples deformed at 10 s$^{-1}$ to that in samples deformed at 0.1 s$^{-1}$, to determine the effect of strain rate on damage. Figure 6(c) shows a micrograph of a sample deformed at 10 s$^{-1}$ to a 0.29 true strain. The damage shown in this micrograph is very similar to that in the sample deformed to a 0.33 strain at 0.1 s$^{-1}$, which is shown in Figure 6(b). Isolated voids were observed, and their dimensions are very similar to those in the sample tested at 0.1 s$^{-1}$. Thus, we conclude that the strain rate in the quasi-static regime did not significantly change the accumulation of damage in samples with equiaxed microstructures.

One sample of the material with the equiaxed microstructure was deformed to a 0.4 true strain at 1 s$^{-1}$ and stopped immediately before the sample had cracked into two pieces. Examination of this sample showed that in three of the four corners of the cross section, macroscopic cracks were growing into the sample along a diagonal line. The cracks in one corner are shown in Figure 7. Although these cracks are much longer than those shown in Figure 6, they are still segmented and only go into the sample a short distance. Therefore, we conclude that significant crack growth only occurs immediately before failure and that prior to that, the voids form and slowly link up into these shorter cracks.

Samples with the Widmanstätten microstructure were sectioned and examined after being deformed to true strains of 0.04, 0.09, 0.15, 0.20, and 0.29 at a strain rate of 0.1 s$^{-1}$. Samples examined with the optical microscope showed no evidence of nonuniform deformation until the strain reached 0.15. At this strain, a few isolated voids were observed. There was also evidence that the Widmanstätten laths and packets of laths rotate as deformation proceeds, so that their long axis becomes parallel to the direction of shear. Figure 8(a) shows an example of this process. Figure 8(b) shows the damage in a sample deformed to a 0.20 strain. Cracks had clearly formed in the material, which were significantly longer than the voids observed in the equiaxed sample strained to 0.29 and 0.33. The depth of penetration can also be observed in Figure 8(c), which is a micrograph taken in a plane normal to the compression axis. The section was at approximately one-third height, and long circumferential cracks are evident. Thus, at this strain, cracks are clearly

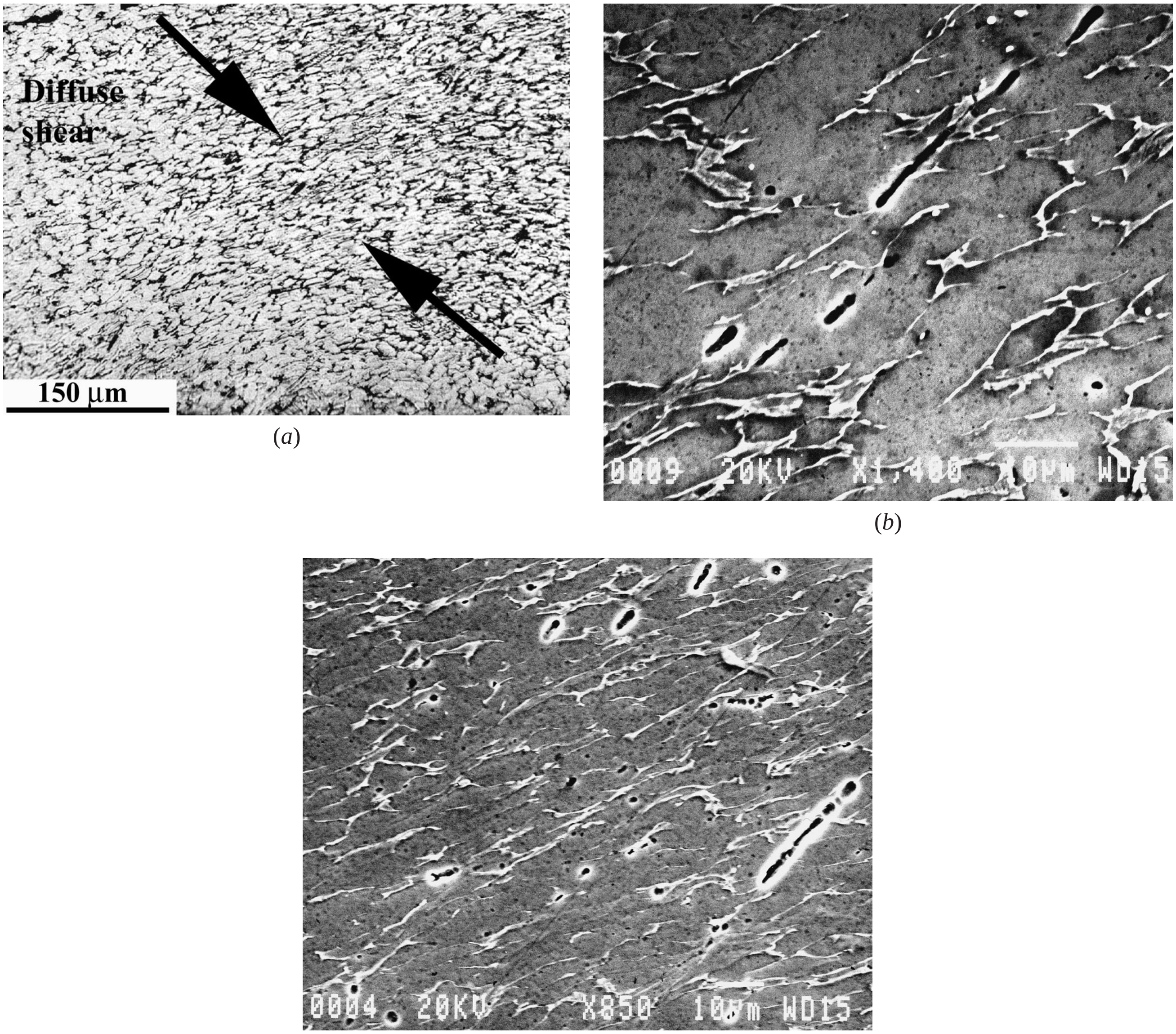


(*a*) (*b*) (*c*)

Fig. 6—An optical micrograph of a sample with the equiaxed microstructure that had been deformed at 0.1 $s^{-1}$ to a true strain of 0.28. Note the area of deformation. (*b*) A scanning electron micrograph showing voids formed in a sample tested at 0.1 $s^{-1}$ to a true strain of 0.33. (*c*) A scanning electron micrograph showing voids formed in a sample tested at 10 $s^{-1}$ to a true strain of 0.29. Note the similarity to the micrograph shown in Fig. (b).

growing into the material along the conical surfaces of the highly deformed material.

Samples of the Widmanstätten microstructure tested at 1 and 10 $s^{-1}$ showed features that were not observed in the equiaxed structure. Figure 9(a) shows an example of a crack that led to failure in a sample tested at 10 $s^{-1}$. Note that the Widmanstätten laths near the crack have been deformed so that they run approximately parallel to the crack. In another sample deformed at 10 $s^{-1}$, the laths next to the main crack are, again, severely deformed, as shown in Figure 9(b). Yet, within 50 $\mu$m of this crack, the microstructure appears to be essentially undeformed. This localized deformation band is suggestive of adiabatic shear bands, but we did not examine the cracked region in sufficient detail to conclusively show that this was the case.

Samples of the equiaxed and Widmanstätten microstructures tested at 1000 $s^{-1}$ to a 0.21 true strain were also examined using the SEM. Figure 10 shows the deformed microstructures of each. There is a region of localized shear in the micrograph of the equiaxed microstructure, as shown in Figure 10(a), which differs from the sheared regions in samples deformed at quasi-static strain rates. At high strain rates, the material surrounding the locally sheared region is left relatively undeformed, and the sheared region is narrow. At the quasi-static strain rates, the sheared regions are typically more diffuse and extend over a larger volume of material, as shown in Figure 6(a). The samples with the Widmanstätten microstructure showed laths aligned and sheared at 45 deg to the loading axis, as also observed at quasi-static strain rates. A few isolated voids and cracks were also observed, and these are visible in Figure 10(b). It is interesting to note that there was no evidence of adiabatic shear banding in any of the samples tested at high strain rates. However, the total strain for these samples was significantly less than that for the quasi-static tests. If we had been able to achieve larger strains, adiabatic shear bands might have been observed. We also found through examination of these samples in the transmission electron microscope that twins were present in the microstructure and were of the $(10\bar{1}2)[\bar{1}011]$ type. This twinning system is one of four known to occur in Ti, and twin formation is typically prevalent in Ti and Ti alloys deformed at high strain rates.[6,21,22] One set of such twins is shown in the bright-field image in Figure 10(c), with the corresponding diffraction pattern on the $[1\bar{2}10]$ zone axis in the inset. The zone axis shown represents the intersection of the $K_1$, or the habit, plane and the $K_2$, or the conjugate twin, plane, and, therefore, the selected-area diffraction pattern appears as a pure rotation about the zone axis. The computer-simulated and indexed pattern is given in Figure 10(d). These twins were not observed in samples deformed at the quasi-static rates.

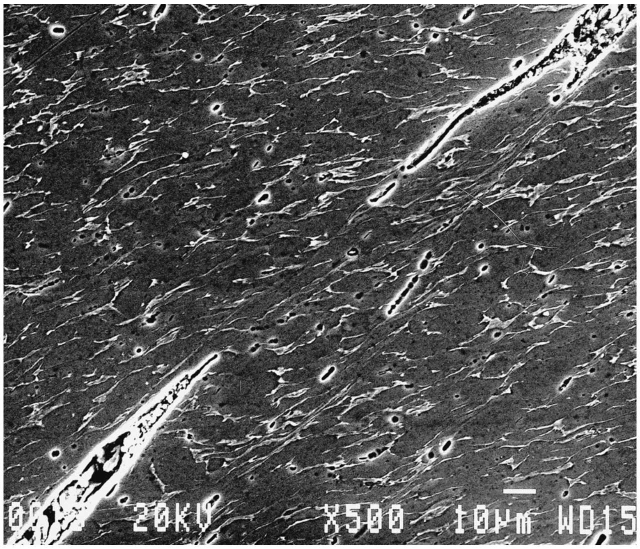


Fig. 7—A scanning electron micrograph of segmented cracks formed in one corner in a sample tested at 0.1 $s^{-1}$ to a true strain of 0.4.

## IV. DISCUSSION

This discussion is divided into three parts. First, we compare our results to others in the literature and explain any differences that have arisen among studies. Second, we explain why the true stress–true strain curve had a maximum at strains less than the failure strain. Last, we discuss why the Widmanstätten structure failed at lower strains that the equiaxed structure.

### A. *Comparison of Yield- and Flow-Stress Results*

Figure 11 shows the yield-stress and flow-stress values from other studies reported in the literature, in which Ti64

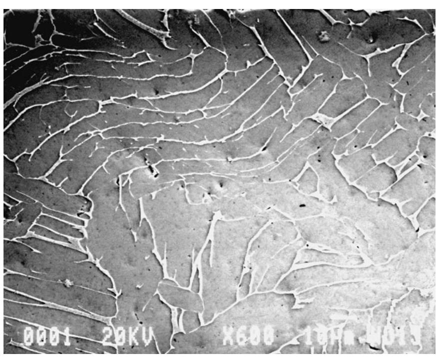


(*a*)

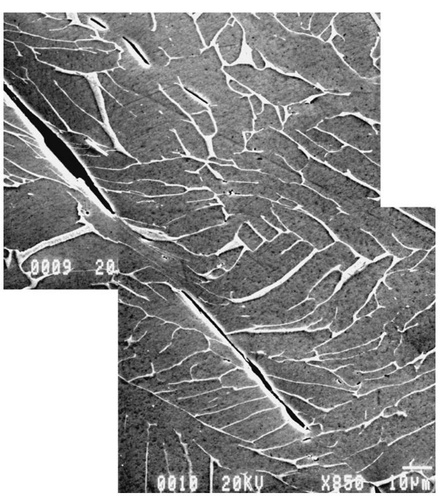


(*b*)


(*c*)

Fig. 8—Microstructures of samples with the Widmanstätten microstructure deformed at 0.1 $s^{-1}$. (*a*) A scanning electron micrograph showing the early stages of lath rotation in a sample deformed to 0.15 true strain. (*b*) Micrograph of a sample deformed to 0.20 strain. (*c*) A scanning electron micrograph of sample deformed to 0.25 true strain. This micrograph was taken in a section perpendicular to the loading axis so that the crack is circumferential.

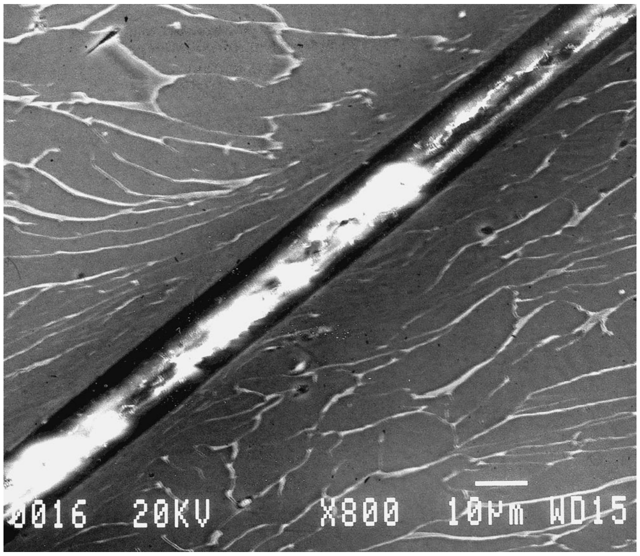


(*a*)

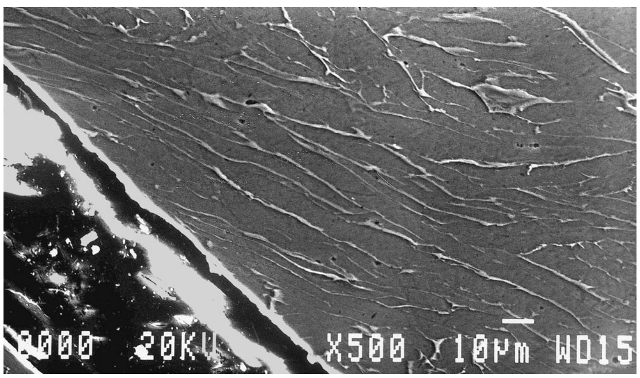


(*b*)

Fig. 9—Cracks in samples with the Widmanstätten, microstructure tested to failure. Note the severe deformation of the laths near the cracks. Samples were deformed at a strain rate of 10 $s^{-1}$.

has been deformed in compression. The results are plotted as a function of strain rate, and individual references are given on the figure, along with the type of microstructure.

Several immediate observations can be made by examining Figure 11. First, the yield and flow stress (at 5 pct plastic strain) appear to be generally independent of microstructure. This point can best be observed in our own study (Figure 3), and the results from other studies do not in any way group themselves by microstructure. Second, we note that the strain-rate dependence of the yield strength and flow stress appears to be similar. The only data that are outside the general trend are those of Kailas *et al.*[7] They reported no strain-rate dependence on the yield strength, and the measured yield strengths were lower than those observed in the other studies.

To investigate further the observed differences in the yield stress and flow stress among the different studies, we considered two possible factors: differences in the grain size and differences in the interstitial level. We now consider each of these in turn.

Grain-size refinement is a well-known strengthening mechanism in metals, but in our study, we found it difficult to change the grain size significantly. A 100-hour heat treatment high in the $\alpha + \beta$–phase field (925 °C) resulted in an increase in the grain size from 8 to 22 $\mu$m, which only decreased the yield strength by 35 MPa. Furthermore, if one examines the results in the literature, there appears to be little correlation between grain size (defined as the grain size for the equiaxed microstructure and lath width for the Widmanstätten microstructure) and yield strength. Figure 12(a) shows a Hall–Petch plot for the literature data for compression tests for which grain size was measured. There is no clear correlation between yield strength and grain size.

Interstitial elements are known to have a strong effect on the yield strength of titanium.[23,24] One way in which to capture the effect of all three common interstitial elements is to use the equivalent oxygen concentration, defined as $O_{eq}$ = [O] + 3/4[C] + 2[N], where square brackets denote concentration in weight percent. We have used that definition and plotted the yield strength as a function of the equivalent oxygen concentration in Figure 12(b). Only data for strain rates less than 1.0 $s^{-1}$ were used to make the plot. Clearly, there is a strong correlation; the yield strength increases with increasing equivalent oxygen concentration. Thus, we conclude that the yield strength and the flow stress at small strains are equivalent for the two microstructures and that the differences in reported values in the literature arise primarily from differences in the interstitial content.

All of the results used to construct the aforementioned plots were taken from studies in which the tests were performed in compression. It is also important to consider the results of two studies[25,26] in which tensile data were obtained on these same two types of microstructures, which had also been prepared from the same parent material. The study by Gysler and Lutjering[25] considered both the effects of grain size and oxygen concentration on the yield stress in tension over a range of temperatures. They found that at room temperature, a change in the equiaxed grain size from 2 to 10 $\mu$m changed the yield stress by approximately 100 MPa. If one assumes that the change in yield stress is linearly related to the inverse square root of the grain size, this change is essentially identical to that which we measured when we varied the grain size from 8 to 22 $\mu$m. Gysler and Lutjering[25] also investigated the effects of oxygen by using two different alloys. Their results are shown in Figure 12(c), which also includes the values for the compression tests that are presented in Figure 12(b). The vertical lines that connect the two points for these two alloys indicate the spread in the yield-strength values that they measured for the different microstructures and different grain sizes. The results appear to agree well with the results from all the compression tests. Also included in Figure 12(c) are the results from Reference 26, which were obtained from tensile tests. Again, the results appear to fit reasonably well with those for obtained from compression tests.

One difference that was noticeable between the studies that examined tensile behavior and our results on compression tests was that the studies that employed tensile testing observed a definite difference in the yield strength of the equiaxed and the Widmanstätten microstructures, whereas we did not. In both of the studies where the samples were tested in tension, the researchers observed that the Widmanstätten structure had a yield strength about 50 MPa below that of the equiaxed structure.[25,26] However, in the compression tests

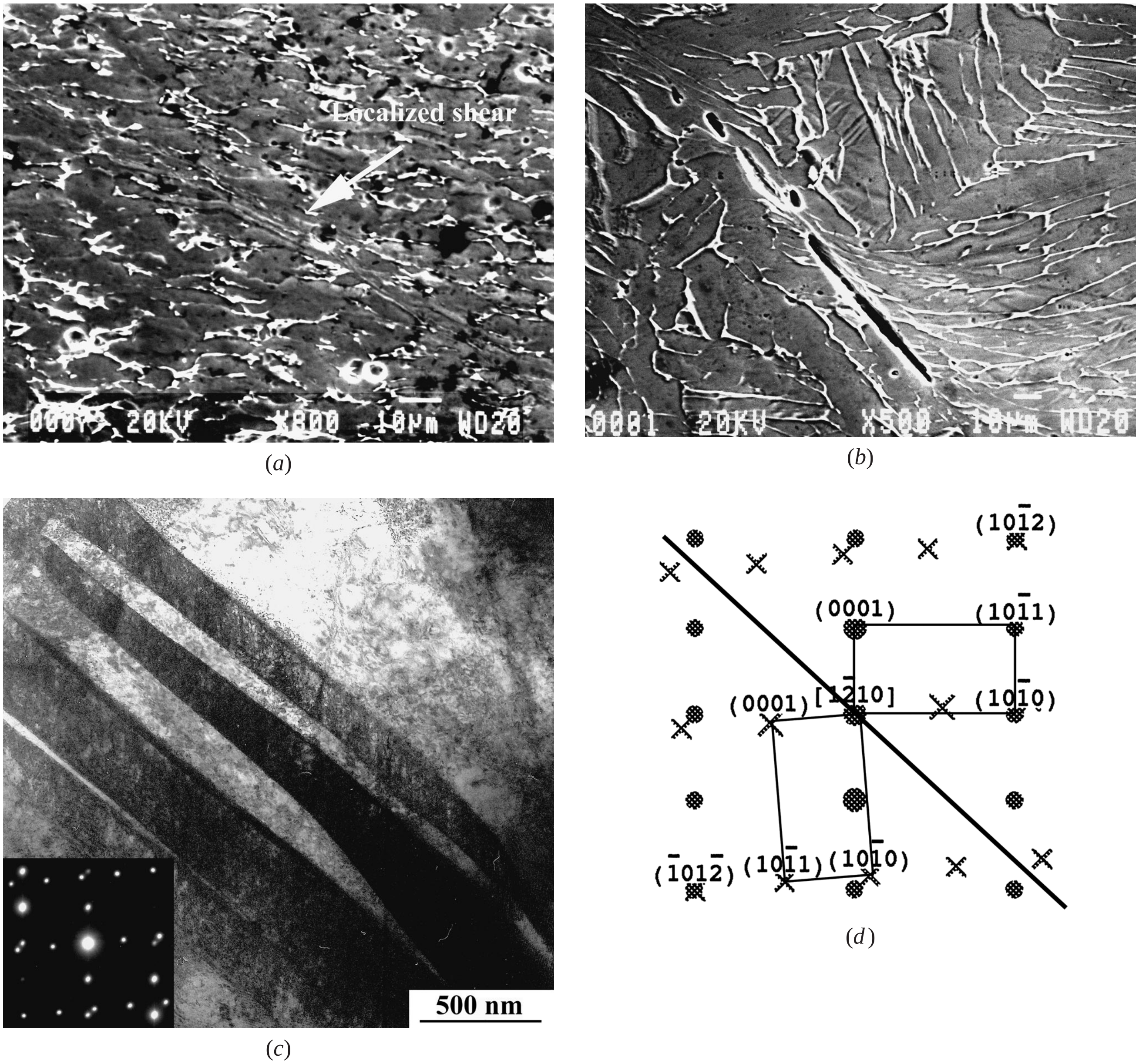


Fig. 10—(*a*) A scanning electron micrograph of a sample with the equiaxed microstructure deformed to 0.21 true strain at 1000 $s^{-1}$. Note the evidence of localized shearing. (*b*) A scanning electron micrograph of a sample deformed to 0.21 true strain at 1000 $s^{-1}$. (*c*) A transmission electron micrograph of twins in a sample deformed at 1000 $s^{-1}$. The sample had the equiaxed microstructure. (*d*) The index of the diffraction pattern shown in the inset in (c).

that we performed, the two microstructures showed essentially identical yield-stress values. At this point, we cannot comment on why this difference might be observed.

### B. *The Maximum in the True Stress–True Strain Curves*

We wanted to investigate why a maximum occurred in the true stress–true strain curve and why this maximum was observed at increasingly lower strains as the strain rate increased. We considered several possibilities. One was that the samples barreled, which would affect the accuracy of the conversion to true stress. However, we did not see any evidence that the amount of barreling changed as a result of changes in microstructure or strain rate, and barreling was as significant at a strain rate of 0.1 $s^{-1}$, where we did not observe the true-stress maximum, as it was at 10 $s^{-1}$, where we did. We also considered the possibility that internal damage (voids or cracks) caused the material softening after the peak stress. However, as shown earlier, the buildup of damage depended on microstructure, but not on strain rate for a given microstructure. The remaining possibility was that the softening beyond a given strain occurred as a result of local heating in the highly deformed part of the sample. We obtained evidence that this heating occurred, and we propose that this is the cause of the material softening at larger strains. We now present this evidence.

We first performed two experiments in which we measured the increase in temperature during deformation by placing a thermocouple in a hole drilled in the side of the sample. One sample was tested at 0.1 $s^{-1}$ and the other at 10 $s^{-1}$.

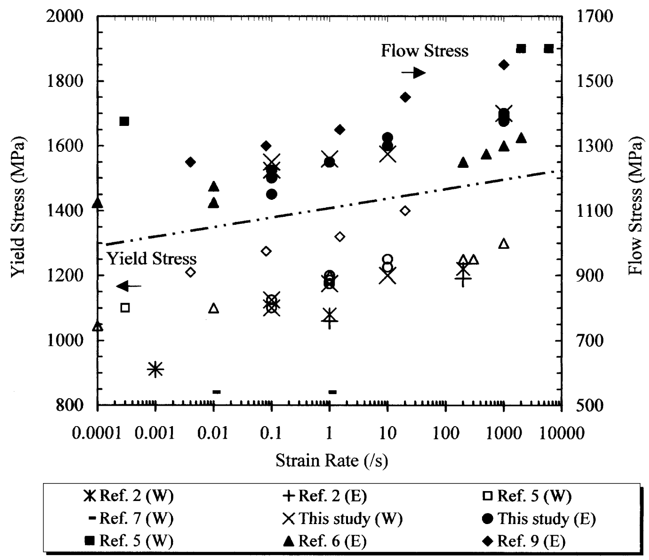


Fig. 11—A summary of the yield and flow stress data obtained from the literature. Open and closed symbols represent the yield and flow stress data, respectively. The dashed line separates the yield and flow stress data. The flow stress values were obtained at either 0.04 or 0.05 true strain. The *E* or *W* after the entry on the legend indicates whether the data are for equiaxed or Widmanstätten microstructures.

A maximum was observed in the true stress–true strain curve when it was tested at the higher of these two strain rates. For the test conducted at 0.1 $s^{-1}$, the temperature remained at 25 °C during elastic deformation and then increased linearly at approximately 53 °C/mm until failure. In the sample deformed at 10 $s^{-1}$, the temperature increased at approximately 175 °C/mm of displacement. This difference in heating rate with deformation is consistent with observing the maximum in true stress at lower strains as the strain rate increases.

An additional experiment was conducted to demonstrate that thermal softening could cause the maximum in true stress. A specimen was deformed to a 0.22 true strain at a strain rate of 10 $s^{-1}$, and then unloaded. This strain would be beyond the true-stress maximum for this strain rate. The sample was allowed to cool, and then it was reloaded at a strain rate of 0.1 $s^{-1}$. Figure 13 shows the load-displacement data obtained from these two compression tests. At 10 $s^{-1}$, the data show a linearly increasing load over approximately 1 mm of displacement, after which the slope of the load-displacement curve, or the material hardening, decreased. A dotted line is drawn on the curve emphasizing this behavior. Upon reloading at 0.1 $s^{-1}$, the hardening behavior is the same as that initially observed in the data for the test at 10 $s^{-1}$. Another line, parallel to the first, is drawn on the data from the test at 0.1 $s^{-1}$ for emphasis. Therefore, after cooling, the sample began to work harden at the original rate. We thus conclude that the maximum in the true stress–true strain curve is primarily caused by thermal softening. We note also that the samples tested at 1000 $s^{-1}$ did not show the true-stress maximum that was observed in the quasi-static regime. One possible interpretation of this difference is that at the high strain rates, the effects of adiabatic heating are observed from the very start of the test. Also, these samples underwent twinning, which could affect the shape of the stress-strain curve.

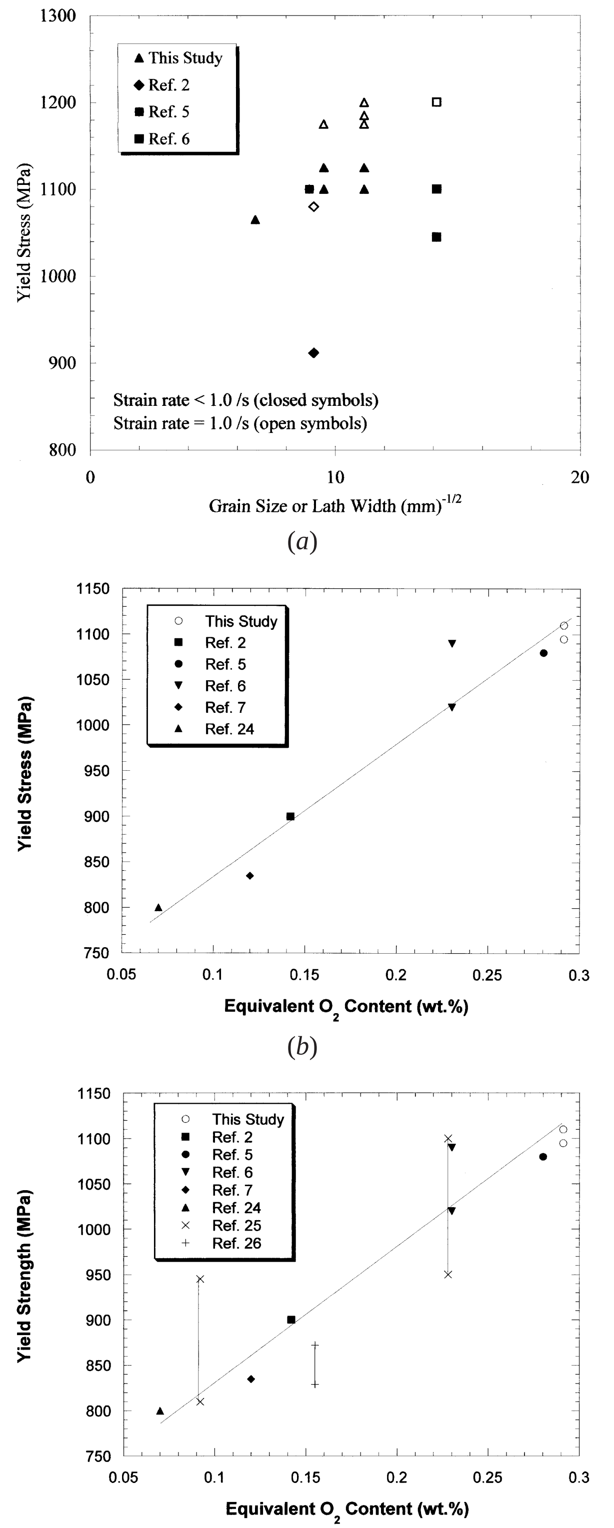


Fig. 12—(*a*) The effect of grain size on yield strength for results reported in the literature. For samples with Widmanstätten microstructures, the lath width was used as a measure of the grain size. (*b*) The effect of interstitial content on the yield stress. The interstitial content is represented by the equivalent oxygen concentration. All results reported in this figure were taken from studies where the yield stress was measured in compression. (*c*) The data in (b) plus results from two studies where yield stress was measured in tension. The vertical lines connect the range of values of yield strength measured in those two studies.[25,26]

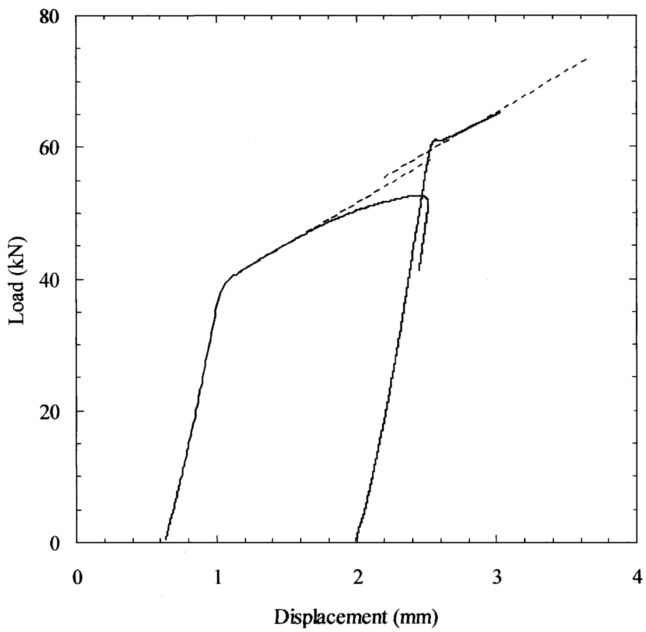


Fig. 13—The measured load plotted as a function of displacement for a specimen first loaded to 20 pct plastic engineering strain at 10 $s^{-1}$ and then reloaded at 0.1 $s^{-1}$. The loading at 10 $s^{-1}$ deformed the sample beyond the maximum in the true stress–true strain curve.

### C. *The Role of Microstructural Morphology in the Failure Process*

The equiaxed and Widmanstätten microstructures exhibited identical yield-stress and flow behaviors at strain rates of 0.1 and 1000 $s^{-1}$ and up to the true-stress maximum at 1.0 and 10 $s^{-1}$. The similarity in behavior at small strains was attributed to the equivalent interstitial content, thermomechanical treatment, and microstructural scale. However, data showed that the failure strains varied significantly between the two microstructures, and results from other studies also suggest that the Widmanstätten microstructure is more susceptible to adiabatic shear-band formation in the quasi-static regime.[5,7]

The failure process in the samples that had the equiaxed microstructure and that were tested at 0.1 $s^{-1}$ can be described as follows. The inhomogeneous deformation initiates in the corners of the specimen and is first visible as regions of diffuse shear, as was shown in Figure 6(a). Next, voids nucleate and grow in the locally sheared regions. For example, the image shown in Figure 6(b) is from a sample deformed to a 0.33 true strain, in which several grains have sheared and a void has initiated in the sheared region. As the process continues, the voids increase in size and in number. Finally, large cracks form by linking the series of voids, and the specimen fails. This sequence appeared to be the process for failure at all quasi-static strain rates that were considered in this study.

The general failure process for samples with the Widmanstätten microstructure can be described as follows. Laths that are preferentially aligned (for example, near 45 deg to the loading axis) and are located near the corners of the specimen begin to rotate such that their long axes align with the direction of shear (Figure 8(a)). As the process continues, the aligned laths shear along their lengths, and other laths may continue to rotate into the direction of shear. Laths that are not preferentially oriented may slow the shearing process of the preferentially aligned laths. In this microstructure, however, voids or small cracks that nucleate in a Widmanstätten lath can grow through the length of the lath. Thus, a much longer crack can initiate in this structure, as compared with the equiaxed structure. In the latter, the crack would be quickly blunted at a grain or phase boundary.

## V. CONCLUSIONS

The results of this study are the following.

1. Samples that had either an equiaxed microstructure or a Widmanstätten microstructure, which had been prepared from the same parent material, showed very similar yield strengths and flow stresses when tested over strain rates of 0.1 to 1000 $s^{-1}$. The yield strength of both microstructures increased with increasing strain rate over this range.
2. The failure strains were lower for the Widmanstätten microstructure at each strain rate, and the difference in the failure strain increased with increasing strain rate in the quasi-static regime. Failure strains were not attained at high strain rates.
3. At strain rates of 1 and 10 $s^{-1}$, local heating during the test caused a maximum in the true stress–true strain curve. This maximum occurred at lower strains with increasing strain rate.
4. The deformation in these samples was typical of that found in compression samples, where friction induces nonuniform deformation. When viewed in a cross section parallel to the loading direction, most deformation was concentrated in two diagonal bands. Voids formed in these diagonal bands and linked up to form macroscopic cracks. This link-up occurred more easily in the lath structure of the Widmanstätten material, which led to the lower fracture strains observed in samples with this microstructure.
5. Examination of other data in the literature showed that the interstitial concentration in the material played a significant role in determining the yield stress.

## ACKNOWLEDGMENTS

This work was primarily supported by the National Science Foundation Sponsored Materials Research Science and Engineering Center, Contract No. DMR-0079964, at Brown University. AWJ was also sponsored by a GANN Fellowship and ASSERT award during the performance of this research. The authors also thank Professor R.J. Clifton for help with the interpretation of the high strain rate tests.

## REFERENCES

1. H.C. Rogers: *Ann. Rev. Mater. Sci.*, 1979, vol. 9, pp. 283-311.
2. L.W. Meyer, L. Krueger, W. Gooch, and M. Burkins: *J. Phys. IV*, 1997, vol. 7 (C3), pp. C3-415-C3-422.
3. S.P. Timothy and I.M. Hutchings: *Acta Metall.*, 1985, vol. 4 (33), pp. 667-76.
4. W.A. Gooch, M.S. Burkins, H.J. Ernst, and T. Wolf: *Lightweight Armour Systems Symp. '95*, 1995, The Royal Military College, Shrivenham, Eng., vol. 110, pp. 1-10.
5. M.G. da Silva and K.T. Ramesh: *Mater. Sci. Eng.*, 1997, vol. A232, pp. 11-22.
6. P.S. Follansbee and G.T. Gray III: *Metall. Trans. A*, 1989, vol. 20A, pp. 863-874.

7. S.V. Kailas, Y.V.R.K. Prasad, and S.K. Biswas: *Metall. Mater. A*, 1994, 25A, pp. 2173-2179.
8. W.S. Lee and M.T. Lin: *J. Mater. Proc. Technol.*, 1997, vol. 71, pp. 235-46.
9. C.J. Maiden and S.J. Greene: *J. Appl. Mech.*, 1966, vol. 33, pp. 496-504.
10. S.C. Liao and J. Duffy: *J. Mech. Phys. Solids*, 1998, vol. 46, pp. 2201-31.
11. T. Seshacharyulu, S.C. Medeiros, J.T. Morgan, J.C. Malas, and W.G. Frazier: *Mater. Sci. Eng.*, 2000, vol. A279, pp. 289-99.
12. P.S. Follansbee: *Metals Handbook*, ASM, Metals Park, OH., 1985. vol. 8, pp. 198-203.
13. G.T. Gray III: *Methods in Materials Research*, John Wiley, New York, NY, 1999.
14. H. Kolsky: *Proc. Phys. Soc. London B*, 1949, vol. 62, pp. 676-700.
15. R.M. Davies: *Phil. Trans. R. Soc. London A*, 1948, vol. 240, pp. 375-457.
16. P.S. Follansbee and C. Frantz: *J. Eng. Mater. Technol.*, 1993, vol. 105, pp. 61-66.
17. D. Banerjee, C.G. Shelton, B. Ralph, and J.C. Williams: *Acta Metall.*, 1988, vol. 36, pp. 125-41.
18. D. Banerjee and J.C. Williams: *Scripta Metall.*, 1983, vol. 17, pp. 1125-28.
19. C.G. Shelton and B. Ralph: *Proc. Congr. The Metallurgy of Light Alloys*, Institute of Metallurgists Conf. No. 20, Institute of Metallurgists, London, 1983, p. 180.
20. C. Hammond and J. Nutting: *Met. Sci.*, 1977, vol. 11, pp. 481-86.
21. S.G. Song and G.T. Gray III: *Metall. Mater. Trans. A*, 1995, vol. 26A, pp. 2665-75.
22. S.G. Song and G.T. Gray III: *Acta Metall. Mater.*, 1995, vol. 43 (6), pp. 2339-50.
23. J. Kratochvil and H. Conrad: *Scripta Metall.*, 1970, vol. 4, pp. 815-24.
24. G. Welsch and W. Bunk: *Metall. Trans. A*, 1982, vol. 13A, pp. 889-99.
25. A. Gysler and G. Lutjering: *Metall. Trans. A*, 1982, vol. 13A, pp. 1435-43.
26. D.-G. Lee, S. Kim, S. Lee, and C.S. Lee: *Metall. Trans. A*, 2001, vol. 32A, pp. 315-24.